

Triplet structure of the nuclear scissors mode

E. B. Balbutsev, I. V. Molodtsova

*Bogoliubov Laboratory of Theoretical Physics, Joint Institute
for Nuclear Research, 141980 Dubna, Moscow Region, Russia*

P. Schuck

*Institut de Physique Nucléaire, IN2P3-CNRS, Université Paris-Sud, F-91406 Orsay Cédex, France;
Univ. Grenoble Alpes, CNRS, LPMMC, 38000 Grenoble, France*

Low energy $M1$ excitations are studied within the Time Dependent Hartree-Fock-Bogoliubov (TDHFB) approach. The solution of TDHFB equations by the Wigner Function Moments method predicts three types of scissors modes. In addition to the conventional scissors mode two new modes arise due to spin degrees of freedom. The lowest one generates a remarkable $M1$ strength below the conventional energy range. The results of calculations for $^{160,162,164}\text{Dy}$ isotopes are compared with experimental data. The puzzle of the ^{164}Dy scissors is explained.

PACS numbers: 21.10.Hw, 21.60.Ev, 21.60.Jz, 24.30.Cz

Keywords: collective motion; scissors mode; spin

I. INTRODUCTION

In this paper, we report on exciting new theoretical and experimental developments concerning nuclear spin scissors modes. In Ref. [1] the Wigner Function Moments (WFM) method was applied for the first time to solve the Time Dependent Hartree-Fock-Bogoliubov equations including spin dynamics. The most remarkable result was the prediction of a new type of nuclear collective motion: rotational oscillations of "spin-up" nucleons with respect of "spin-down" nucleons (the spin scissors mode). This new type of nuclear scissors complements the conventional (orbital) scissors mode. Later, promising experimental traces of this were found in Actinides and some Rare Earth nuclei [2].

The scissors mode is defined as a rotational mode of isovector character. That is why we had divided (approximately) the dynamical equations describing collective motion into isovector and isoscalar parts with the aim to separate the pure scissors mode. In this way we achieved satisfactory agreement with the experimental data obtained by the Nuclear Resonance Fluorescence (NRF) experiments [2]. However, the nuclei considered have more neutrons than protons and, thus, Isospin is not a good quantum number. Therefore, to test the decoupling-approximation used earlier, we solved the coupled dynamical equations for protons and neutrons exactly, without the artificial isovector-isoscalar decoupling. As a surprising result one more magnetic mode (third type of scissors) appeared. Actually, the existence of three scissors states is naturally explained by combinatorics – there are only three ways to divide the four different kinds of objects (spin up and spin down, protons and neutrons in our case) into two pairs, namely: i) spin-up and spin-down protons oscillate versus the corresponding neutrons (the standard scissors mode) ii) protons and neutrons, both spin-up oscillate ver-

sus same with spin-down iii) protons spin-up with neutrons spin-down oscillate versus protons spin-down with neutrons spin-up. We will detail our approach in this paper and compare with very new experimental data of the Oslo group [3].

II. MODEL AND WFM METHOD

The TDHFB equations in matrix formulation are [4, 5]

$$i\hbar\dot{\mathcal{R}} = [\mathcal{H}, \mathcal{R}], \quad (1)$$

with

$$\mathcal{R} = \begin{pmatrix} \hat{\rho} & -\hat{\kappa} \\ -\hat{\kappa}^\dagger & 1 - \hat{\rho}^* \end{pmatrix}, \quad \mathcal{H} = \begin{pmatrix} \hat{h} & \hat{\Delta} \\ \hat{\Delta}^\dagger & -\hat{h}^* \end{pmatrix}. \quad (2)$$

The normal density matrix $\hat{\rho}$ and Hamiltonian \hat{h} are hermitian whereas the abnormal density $\hat{\kappa}$ and the pairing gap $\hat{\Delta}$ are skew symmetric: $\hat{\kappa}^\dagger = -\hat{\kappa}^*$, $\hat{\Delta}^\dagger = -\hat{\Delta}^*$.

The microscopic Hamiltonian of the model, harmonic oscillator with spin-orbit potential plus separable quadrupole-quadrupole and spin-spin residual interactions is given by

$$\hat{h} = \sum_{i=1}^A \left[\frac{\hat{\mathbf{p}}_i^2}{2m} + \frac{1}{2}m\omega^2 \mathbf{r}_i^2 - \eta \hat{\mathbf{l}}_i \hat{\mathbf{S}}_i \right] + H_{qq} + H_{ss}, \quad (3)$$

with

$$\begin{aligned} H_{qq} &= \sum_{\mu=-2}^2 (-1)^\mu \left\{ \bar{\kappa} \sum_i^Z \sum_j^N + \frac{\kappa}{2} \left[\sum_{i,j(i \neq j)}^Z + \sum_{i,j(i \neq j)}^N \right] \right\} \\ &\quad \times q_{2-\mu}(\mathbf{r}_i) q_{2\mu}(\mathbf{r}_j), \\ H_{ss} &= \sum_{\mu=-1}^1 (-1)^\mu \left\{ \bar{\chi} \sum_i^Z \sum_j^N + \frac{\chi}{2} \left[\sum_{i,j(i \neq j)}^Z + \sum_{i,j(i \neq j)}^N \right] \right\} \\ &\quad \times \hat{S}_{-\mu}(i) \hat{S}_\mu(j) \delta(\mathbf{r}_i - \mathbf{r}_j), \end{aligned}$$

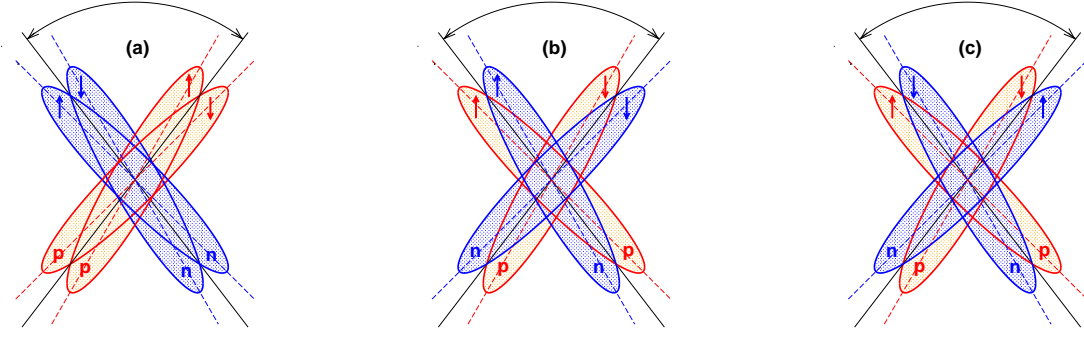


FIG. 1: Schematic representation of three scissors modes: (a) spin-scalar isovector (conventional, orbital scissors), (b) spin-vector isoscalar (spin scissors), (c) spin-vector isovector (spin scissors). Arrows show the direction of spin projections; p – protons, n – neutrons. The small angle spread between the various distributions is only for presentation purposes. In reality the distributions are perfectly overlapping.

where $q_{2\mu}(\mathbf{r})$ is a quadrupole operator, \hat{S}_μ are spin matrices [6], κ , $\bar{\kappa}$ and χ , $\bar{\chi}$ are strength constants, N and Z – numbers of neutrons and protons respectively.

With the help of Fourier (Wigner) transformation the equations (1) are transformed into TDHFB equations for functions $f^{\tau\varsigma}(\mathbf{r}, \mathbf{p}, t)$ and $\kappa^{\tau\varsigma}(\mathbf{r}, \mathbf{p}, t)$ (Wigner transforms of $\hat{\rho}$ and $\hat{\kappa}$), where τ is the isospin index, $\varsigma = +, -, \uparrow\downarrow, \downarrow\uparrow$ is the spin index, and $f^\pm = f^\uparrow \pm f^\downarrow$. Integrating these equations over the phase space with the weights 1, $\{r \otimes r\}_{\lambda\mu}$, $\{p \otimes p\}_{\lambda\mu}$, $\{r \otimes p\}_{\lambda\mu}$, where $\{r \otimes p\}_{\lambda\mu} = \sum_{\sigma,\nu} C_{1\sigma,1\nu}^{\lambda\mu} r_\sigma p_\nu$ and $C_{1\sigma,1\nu}^{\lambda\mu}$ is a Clebsch-Gordan coefficient [6], one gets dynamical equations for the following second order moments, that is collective variables:

$$\begin{aligned} F^{\tau\varsigma}(t) &= (2\pi\hbar)^{-3} \int d\mathbf{p} \int d\mathbf{r} f^{\tau\varsigma}(\mathbf{r}, \mathbf{p}, t), \\ R_{\lambda\mu}^{\tau\varsigma}(t) &= (2\pi\hbar)^{-3} \int d\mathbf{p} \int d\mathbf{r} \{r \otimes r\}_{\lambda\mu} f^{\tau\varsigma}(\mathbf{r}, \mathbf{p}, t), \\ P_{\lambda\mu}^{\tau\varsigma}(t) &= (2\pi\hbar)^{-3} \int d\mathbf{p} \int d\mathbf{r} \{p \otimes p\}_{\lambda\mu} f^{\tau\varsigma}(\mathbf{r}, \mathbf{p}, t), \\ L_{\lambda\mu}^{\tau\varsigma}(t) &= (2\pi\hbar)^{-3} \int d\mathbf{p} \int d\mathbf{r} \{r \otimes p\}_{\lambda\mu} f^{\tau\varsigma}(\mathbf{r}, \mathbf{p}, t), \\ \tilde{R}_{\lambda\mu}^{\tau\varsigma}(t) &= (2\pi\hbar)^{-3} \int d\mathbf{p} \int d\mathbf{r} \{r \otimes r\}_{\lambda\mu} \kappa^{\tau\varsigma}(\mathbf{r}, \mathbf{p}, t), \\ \tilde{P}_{\lambda\mu}^{\tau\varsigma}(t) &= (2\pi\hbar)^{-3} \int d\mathbf{p} \int d\mathbf{r} \{p \otimes p\}_{\lambda\mu} \kappa^{\tau\varsigma}(\mathbf{r}, \mathbf{p}, t), \\ \tilde{L}_{\lambda\mu}^{\tau\varsigma}(t) &= (2\pi\hbar)^{-3} \int d\mathbf{p} \int d\mathbf{r} \{r \otimes p\}_{\lambda\mu} \kappa^{\tau\varsigma}(\mathbf{r}, \mathbf{p}, t). \end{aligned} \quad (4)$$

There are 44 coupled isovector and isoscalar equations of the first order in time, which can be reduced to 22 equations of the second order in time. Excluding the integrals of motion we obtain 14 eigenvalue solutions. The coupling constants are as in our previous publications [1, 2, 7].

III. RESULTS OF CALCULATIONS AND DISCUSSION

First, the results of our calculations for ^{164}Dy are presented in the Table I, where the energies, magnetic dipole and electric quadrupole strengths are shown in the energy range $0 \leq E \leq 4$ MeV. Left panel – the solutions of decoupled equations, right – isoscalar-isovector coupling is taken into account. Comparing

TABLE I: The results of WFM calculations for ^{164}Dy : energies E [MeV], magnetic dipole $B(M1)$ [μ_N^2] and electric quadrupole $B(E2)$ [W.u.] strengths. IS – isoscalar, IV – isovector.

	Decoupled equations			Coupled equations		
	E	$B(M1)$	$B(E2)$	E	$B(M1)$	$B(E2)$
IS	1.29	0.01	53.25	1.47	0.17	25.44
IV	2.44	2.03	0.34	2.20	1.76	3.30
IS	2.62	0.09	2.91	2.87	2.24	0.34
IV	3.35	1.36	1.62	3.59	1.56	4.37

the left and right panels, we see that the most remarkable change happens with the third low-lying level, an isoscalar one without coupling, – it acquires a rather big magnetic strength. So, in the decoupled case there are 2 isoscalar electric and 2 isovector magnetic low-lying levels, and in the coupled case there are 1 electric and 3 magnetic levels of mixed isovector-isoscalar nature. The lowest electric level can be interpreted as the relative oscillations of the total orbital angular momentum versus the total nucleus' spin [7]. Such a motion surely seems possible but for the moment we have not investigated this motion more deeply nor have we much searched for an experimental equivalence. It is a task for the future.

The three magnetic states correspond to three physically possible types of scissors modes already mentioned in the introduction. The state at the energy of 3.59 MeV is the conventional "orbital" scissors mode, the last two states at the energies of 2.20 MeV and 2.87

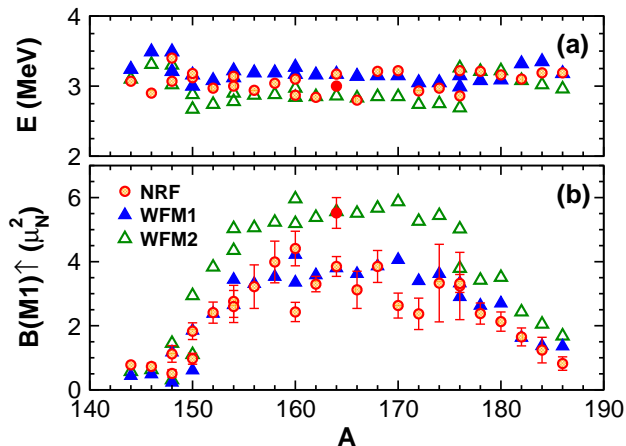


FIG. 2: Calculated (WFM) and experimental (NRF) mean excitation energies (a) and summed $M1$ strengths (b) of the scissors mode. WFM1 – the sum of two highest scissors, WFM2 – the sum of three scissors. Experimental data are taken from the papers listed in the Table 1 of [9]. The solid circle marks the experimental result for ^{164}Dy when summed in the energy range from 2 to 4 MeV.

MeV are the "spin" scissors modes. As follows from our calculations, the spin scissors are lower in energy and stronger in transition probability than the orbital scissors. The Fig. 1 shows a schematic representation of these modes: the orbital scissors (neutrons versus protons) and two spin scissors (spin-up nucleons versus spin-down nucleons and more complicated – spin-up protons together with spin-down neutrons versus spin-down protons with spin-up neutrons). Both spin scissors exist only due to spin degrees of freedom. If we remove the arrows from the picture, nothing will change for the conventional scissors (a). However figures (b) and (c) in this case become identical and senseless, because the division of neutrons and protons in two parts becomes irrelevant.

Our previous calculations [1, 2, 7] were performed in the approximation of isovector-isoscalar decoupling. We have found that with the help of the two above mentioned low lying magnetic states (left panel of Table I) one is able to obtain rather good agreement with experimental data on low lying 1^+ states in Actinides and Rare Earth nuclei.

Calculations without an artificial decoupling produce three low lying magnetic states (instead of two without coupling), see Table I, whose summarized magnetic strength $\sum B(M1) = 5.56 \mu_N^2$ is remarkably stronger than the analogous value $\sum B(M1) = 3.39 \mu_N^2$ of two magnetic states in the case of decoupling. One would say that it is also stronger than the respective experimental value. However, one must be careful here.

Trying to compare the theoretical results with the existing experimental data for the scissors mode, we encounter different summing interval conventions. It is assumed that scissors mode includes only the states

in a certain energy range. As a rule, the following two conventions are chosen, which lead to slightly different results for the summed $M1$ strength:

$$\begin{aligned} 2.7 < E < 3.7 \text{ MeV for } Z < 68 \text{ and} \\ 2.4 < E < 3.7 \text{ MeV for } Z \geq 68 \text{ [8],} \\ 2.5 < E < 4.0 \text{ MeV for } 82 \leq N \leq 126 \text{ [9].} \end{aligned}$$

Obviously, only two highest scissors fall into both of these intervals. It turns out that their summed $B(M1)$ agrees rather well with the majority of experimental values found by NRF experiments [8, 9] for nuclei of $N = 82 - 126$ mass region (see Fig. 2). The situation with the lowest scissors is very interesting. It helps to explain the long-standing problem of the 1^+ spectrum of ^{164}Dy .

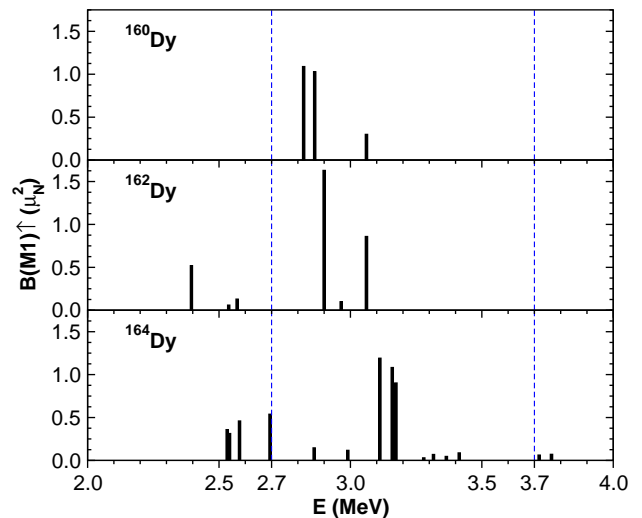


FIG. 3: Excitation energies E with the corresponding $B(M1)$ values, obtained by the NRF experiment [10]. The dashed lines mark the boundaries of the conventional interval from [8].

The Fig. 3 demonstrates experimental $M1$ strength distributions in $^{160,162,164}\text{Dy}$ in the energy range between 2 and 4 MeV, reported by Margraf *et al.* [10]. Obviously, there are two groups of strong $M1$ excitations in ^{164}Dy around 2.6 and 3.1 MeV. However, only the upper group was attributed to the scissors mode, and the group around 2.6 MeV was not included because their summed $M1$ strength strongly deviates from the scissors mode systematics in the Rare Earth nuclei [9]. The results of our calculations allows one to clarify the origin of both groups. Table II demonstrates that the energy centroid and summed $B(M1)$ -value of the lower group agree very well with the calculated E and $B(M1)$ of the lowest scissors. The respective values of the higher group are in excellent agreement with the energy centroid and summed $B(M1)$ of two remaining (higher in energy) scissors.

So, according to our calculations, the low-energy group of states in ^{164}Dy is also a branch of the scissors mode (spin-vector isovector scissors).

In the rest nuclei of $N = 82 - 126$ mass region an equally significant low energy $M1$ strength was not de-

TABLE II: The energies E [MeV] and excitation probabilities $B(M1)$ [μ_N^2] of three scissors are compared with experimental values \bar{E} and $\sum B(M1)$ of two groups of 1^+ levels in ^{164}Dy [10].

Theory (WFM)				Experiment (NRF)	
E	$B(M1)$	\bar{E}	$\sum B(M1)$	\bar{E}	$\sum B(M1)$
2.20	1.76	2.20	1.76	2.60	1.67(14)
2.87	2.24	3.17	3.80	3.17	3.85(31)
3.59	1.56				

tected in the NRF experiments. However, our calculations predict the existence of comparable magnetic strength in all well-deformed nuclei of this mass region (see WFM2 in Fig. 2). This prediction is supported by calculations [11, 12] in the frame of Quasiparticle-Phonon Nuclear Model (QPNM), which also predicts remarkable $M1$ strength below the conventional energy interval (see Table III).

Our prediction is also supported by the recent experimental results of photo-neutron measurements performed by the Oslo group. In Ref. [3] the authors revised their previous data on the scissors resonance (SR) in $^{160-164}\text{Dy}$ obtained by the Oslo method. The essence of their findings is formulated in the following quotation from [3]: “...If we integrate over all transition energies, we find a total, summed SR strength of $4 - 5 \mu^2$. The present fit strategy gives about 40% higher summed SR strengths than the reported NRF results. However, if we apply the NRF energy limits, we obtain excellent agreement with the NRF results. It is interesting to note that $\sim 40 - 60\%$ of our measured SR strength lies in the energy region below 2.7 MeV. In traditional NRF experiments using bremsstrahlung, the transitions in this energy range are quite difficult to separate from the sizable atomic background.”

This is exactly the point! The statements about “40% higher” and “ $\sim 40 - 60\%$... below 2.7 MeV” are in perfect agreement with our findings!

The energy centroids and corresponding summed $B(M1)$ given by the WFM theory and by the QPNM calculations [11, 12] are compared with experimental results from the NRF and from photo-neutron measurements (Oslo) [3] in Table III. The results are shown for various energy averaging intervals. As it is seen, the theoretical results and experimental data of Oslo group are in very good overall agreement for all three Dy isotopes. It is worthwhile to remark the excellent agreement between all theoretical and experimental results for ^{164}Dy . One may be worried by the comparatively big interval $0 < E < 10$ MeV employed by the Oslo group [3] for centroids energies and $B(M1)$. However, in their paper they say that they eliminated all spin-flip excitations in their averages and, thus, their averaging becomes equal to the theoretical one, since it is generally believed that all what is above 4 MeV excitation energy does not belong to

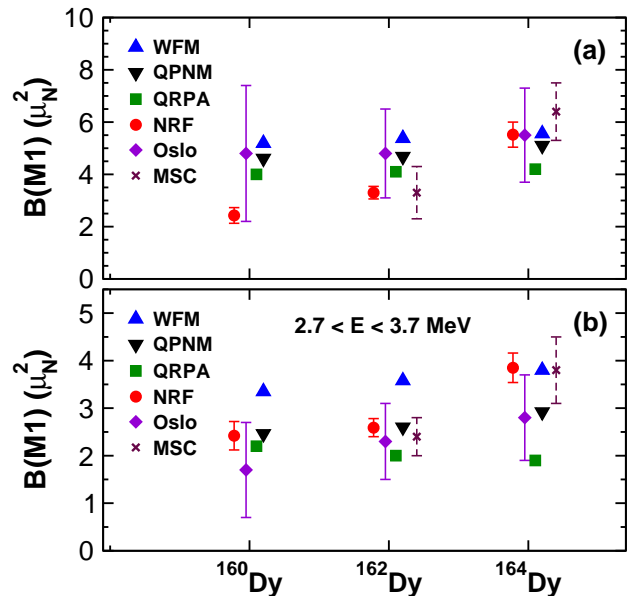


FIG. 4: Comparison of the summed $B(M1)$ values for SR in $^{160,162,164}\text{Dy}$ from the present WFM theory, the QPNM [11, 12] and Gogny QRPA [3] calculations with the experimental values from the NRF [10], photo-neutron measurements (Oslo) [3] and from multistep-cascade (MSC) measurements of γ decay following neutron capture [13]. Panel (a) – averaging energy intervals are 2 – 4 MeV for WFM and NRF; 0 – 3.5 MeV for QRPA; 0 – 10 MeV for Oslo and MSC; see Table III for QPNM, (b) – averaging interval is 2.7 – 3.7 MeV.

SR excitations. In Fig. 4 the averages for $B(M1)$ values are also shown for $^{160,162,164}\text{Dy}$ including this time the results from Gogny QRPA calculations and the experimental results obtained by the radiative capture of resonance neutrons [13]. It is remarkable to which extent theory and experiment agree taking the NRF as well as the Oslo averaging intervals. This yields strong support to our interpretation that there are in fact not one but three intermingled scissors modes at play: the standard one and two spin scissors which may be predominately isovector spin-vector and isoscalar spin-vector in nature. As mentioned, this is just the natural triplet of scissors modes which one obtains from pure combinatorics.

The case of Actinides is similar to the Rare Earth region. It will be discussed in an extended version of the paper to be published.

IV. CONCLUSION

We have solved the dynamical equations describing the nuclear collective motion without the division into isovector and isoscalar parts, an approximation we had applied in our previous work. As a result a new, third, type of nuclear scissors is found. The three types of scissors modes can be approximately classi-

TABLE III: The energy centroids \bar{E} [MeV] and corresponding summed $B(M1)$ [μ_N^2] values given by WFM theory and QPNM calculations [11, 12] are compared with experimental results by the NRF [10] and photo-neutron measurements (Oslo) [3] for $^{160,162,164}\text{Dy}$. Comparison is presented for various energy intervals.

^ADy	Theory			Experiment			
	WFM		QPNM	NRF		Oslo	
	\bar{E}	$B(M1)$	$B(M1)$	\bar{E}	$B(M1)$	\bar{E}	$B(M1)$
	$2.7 < E < 3.7$ MeV			$2.7 < E < 3.7$ MeV			
^{160}Dy	3.17	3.35	2.46	2.87	2.42(30)	2.66(12)	1.7(10)
^{162}Dy	3.16	3.58	2.60	2.96	2.59(19)	2.81(8)	2.3(8)
^{164}Dy	3.17	3.80	2.92	3.17	3.85(31)	2.83(8)	2.8(9)
	$2.0 < E < 3.7$ MeV			$2.0 < E < 4.0$ MeV		$0 < E < 10$ MeV	
^{160}Dy	2.84	5.19	4.61	2.87	2.42(30)	2.66(12)	4.8(26)
^{162}Dy	2.85	5.38	4.68	2.84	3.30(24)	2.81(8)	4.8(17)
^{164}Dy	2.86	5.56	5.10 ^a	3.00	5.52(48)	2.83(8)	5.5(18)

^aThe summing energy range is $2.0 < E < 3.9$ MeV [12].

fied as isovector spin-scalar (conventional), isovector spin-vector and isoscalar spin-vector, see Fig. 1. The calculated energy centroids and summarized transition probabilities of even-even Dy isotopes are in very good agreement with the experimental results of the Oslo group. The experimental NRF data for ^{164}Dy are also in excellent agreement with our calculations, whereas the data for $^{160,162}\text{Dy}$ are in good agreement only with the calculated centroids of the two higher lying scissors. So we agree with the conclusion of the authors of [3]: “It is highly desirable to remeasure the Dy isotopes by performing NRF experiments using quasi-

monochromatic beams in the interesting energy region between 2 and 4 MeV as done for ^{232}Th .” According to our latest findings it is necessary to extend their proposal to all Rare Earth and Actinide nuclei.

Acknowledgments

We thank S. Péru-Desenfants for collaboration and discussion. This work was supported by the IN2P3/CNRS-JINR 03-57 Collaboration agreement.

-
- [1] E. B. Balbutsev, I.V. Molodtsova, P. Schuck, Phys. Rev. C 91 (2015) 064312.
 - [2] E. B. Balbutsev, I.V. Molodtsova, P. Schuck, Phys. Rev. C 97 (2018) 044316.
 - [3] T. Renstrøm, H. Utsunomiya, H. T. Nyhus, A. C. Larsen, M. Guttormsen, G. M. Tveten, D. M. Filipescu, I. Gheorghe, S. Goriely, S. Hilaire, Y.-W. Lui, J. E. Midtbø, S. Péru, T. Shima, S. Siem, O. Tesileanu, Phys. Rev. C 98 (2018) 054310.
 - [4] V. G. Soloviev, *Theory of complex nuclei* (Pergamon Press, Oxford, 1976).
 - [5] P. Ring and P. Schuck, *The Nuclear Many-Body Problem* (Springer, Berlin, 1980).
 - [6] D. A. Varshalovitch, A. N. Moskalev, V. K. Khersonski, *Quantum Theory of Angular Momentum* (World Scientific, Singapore, 1988).
 - [7] E. B. Balbutsev, I.V. Molodtsova, P. Schuck, Nucl. Phys. A 872 (2011) 42.
 - [8] N. Pietralla, P. von Brentano, R.-D. Herzberg, U. Kneissl, J. Margraf, H. Maser, H. H. Pitz, A. Zilges, Phys. Rev. C 52 (1995) R2317.
 - [9] J. Enders, P. von Neumann-Cosel, C. Rangacharyulu, A. Richter, Phys. Rev. C 71 (2005) 014306.
 - [10] J. Margraf, T. Eckert, M. Rittner, I. Bauske, O. Beck, U. Kneissl, H. Maser, H. H. Pitz, A. Schiller, P. von Brentano, R. Fischer, R.-D. Herzberg, N. Pietralla, A. Zilges, H. Friedrichs, Phys. Rev. C 52 (1995) 2439.
 - [11] V. G. Soloviev, A. V. Sushkov, N. Yu. Shirikova, Phys. Part. Nucl. 31(4) (2000) 385.
 - [12] V. G. Soloviev, A. V. Sushkov, N. Yu. Shirikova, N. Lo Iudice, Nucl. Phys. A 600 (1996) 155.
 - [13] S. Valenta, B. Baramsai, T. A. Bredeweg, A. Couverture, A. Chyzh, M. Jandel, J. Kroll, M. Krťička, G. E. Mitchell, J. M. O'Donnell, G. Rusev, J. L. Ullmann, C. L. Walker, Phys. Rev. C 96 (2017) 054315.